

Antibacterial Potential of Novel Acetamide Derivatives of 2-Mercaptobenzothiazole: Synthesis and Docking Studies

Ahmed Sadiq Sheikh, Humaira Nadeem,* Muhammad Tariq Khan, Adil Saeed, and Babar Murtaza



Cite This: *ACS Omega* 2023, 8, 9785–9796



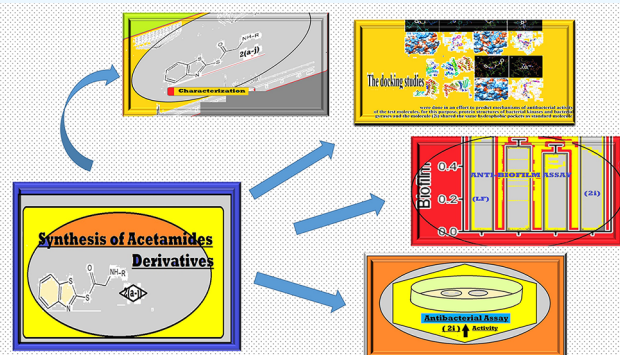
Read Online

ACCESS |

Metrics & More

Article Recommendations

ABSTRACT: 2-Mercaptobenzothiazole and its derivatives are widely known for their diverse biological activities, particularly antimicrobial and anticancer potential. In the present study, a series of new hybrid compounds consisting of 2-mercaptobenzothiazole and different aryl amines **2(a–j)** were synthesized and characterized by Fourier transform infrared (FTIR), ^1H NMR, and ^{13}C NMR spectral data. The synthesized compounds were screened for *in vitro* antibacterial activities through agar well diffusion assay. Among the series, **2b**, **2c**, and **2i** exhibited significant antibacterial activity comparable to the standard drug levofloxacin. Based on their antibacterial potential, these compounds were further tested for their antibiofilm activity. All of the three compounds showed promising antibiofilm potential, even better than the standard drug cefadroxil at $100\ \mu\text{g}/100\ \mu\text{L}$ concentration. Molecular docking studies were performed to explore the antibacterial mechanism of these compounds. Strikingly, the molecule **2i** shared the same hydrophobic pockets as those of levofloxacin in case of bacterial kinases and DNA gyrases. In addition, **2i** exhibited satisfactory antibiofilm activity in comparison to the standard. Our study therefore suggested that the synthetic compound **2i** possesses remarkable antibacterial activity and may serve as a lead molecule for the discovery of potent antibacterial agents.



1. INTRODUCTION

In recent years, the concept of hybrid molecules that contain two or more pharmacophore groups bound together covalently in one molecular framework has been introduced. It has been suggested that such compounds may inhibit two or more conventional targets simultaneously. This multiple target strategy has already resulted in the development of a number of bioactive hybrid molecules.¹ Multicomponent reactions with at least three components in the one-pot process to give a single product represent a unique strategy that leads to the formation of multiple bioactive molecules due to its convergence, low energy consumption, minimum waste generation, simple design, high selectivity, and productivity.² These compounds and their derivatives may have diverse and effective biological activities. The significance of coupling amines with heterocycles, especially 2-mercaptobenzothiazole and related compounds, has been well established, as illustrated by the large number of patents as chemotherapeutic agents.³ On the other side, a number of heterocyclic amines have been reported to exhibit anti-inflammatory,⁴ antileishmanial,⁵ antidiabetic,⁶ antioxidant,⁷ anticancer,⁸ and, most importantly, antimicrobial⁹ activities. Therefore, the synthesis of hybrid molecules incorporating different bioactive scaffolds is highly preferred in the field of drug discovery. The initial step in the designing of dual-acting molecules is that of

searching for collections of biologically active molecules to design pharmacophores' coupling.¹⁰ It ultimately grasps effective compounds with the aim of targeting different enzymes in the biochemical pathway. It is worth mentioning that 2-mercaptobenzothiazole is a privileged heterocyclic scaffold with multiple applications and a tremendous range of pharmacological activity.¹¹ 2-Mercaptobenzothiazole derivatives with an additional thiol moiety have proven to be a novel class of therapeutic agents that possess a number of biological effects such as antiviral,¹² anti-inflammatory,¹³ antileishmanial activities,¹⁴ antidiabetic,¹⁵ anticancer,¹⁶ and antibacterial.¹⁷

The increased number of infectious diseases and the emergence of multi-drug-resistant bacteria are two of the greatest challenges to the human race.¹⁸ The overutilization of the common antimicrobial agents has triggered the emergence of resistant bacteria, causing the diminished efficiency of these moieties.¹⁹ Extensive studies of antimicrobial resistance have

Received: September 6, 2022

Accepted: March 1, 2023

Published: March 9, 2023



Scheme 1. General Scheme for the Synthesis of Acetamide 2-Mercaptobenzothiazole Derivatives

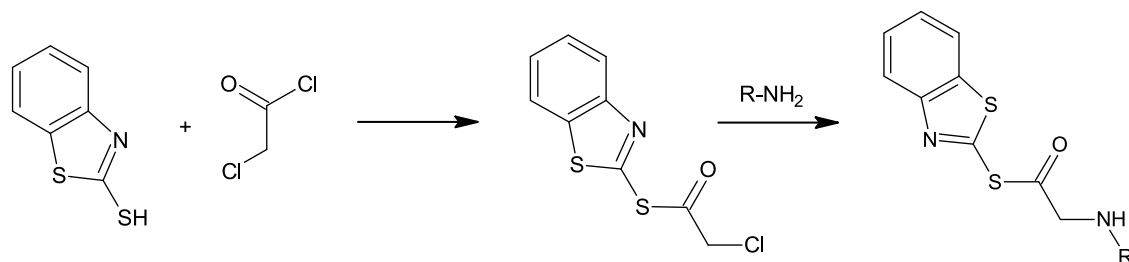


Table 1. Synthesized Acetamide 2-Mercaptobenzothiazole Derivatives 2(a–j)

No.	Code	Substrate (R)	Product	Yield (%)
1	2a			88
2	2b			83
3	2c			77
4	2d			75
5	2e			81
6	2f			69
7	2g			83
8	2h			75
9	2i			70
10	2j			76

revealed that resistant bacterial infections are developed not only due to free bacteria but also due to bacteria existing within a biofilm.²⁰ Biofilm-forming bacteria become resistant to conventional antimicrobials due to (1) the failure of the antimicrobial to go through the biofilm, (2) development of complex drug resistance properties, and (3) biofilm-mediated inactivation or alteration of antimicrobial enzymes.²¹ The biofilm is an important virulence factor for a number of bacterial strains due to its resistance to available antibacterial therapy. It also limits the penetration of antibacterial agents through the matrix and protects the cells from host immune responses. As the biofilm confers a beneficial nature to pathogens, especially in the process of colonization on medical

devices or patient organs, it provides the bacteria more tolerance and strength to exogenous stress including anti-infectious agents, thus making them resistant. This rapid rise in antimicrobial drug resistance has created severe public health issues and has encouraged the researchers to synthesize novel drugs to overcome the resistance to antimicrobial agents and improve therapeutic properties and tolerability with lesser side effects. Hence, there is an urgent need to develop newer and effective molecules with a high safety profile.^{22,23}

1.1. Study Rationale. It has been observed from the literature that sulfur is unusually common in many antimicrobial drugs; therefore, sulfur-containing heterocycles are being explored widely. Interestingly, the introduction of

Table 2. Antibacterial Activity of Compounds 2(a–j)^a

Sr. No.	codes	inhibition zone of bacterial growth (mm)					
		Gram (–) bacteria			Gram (+) bacteria		
		<i>Klebsiella pneumoniae</i> ATCC 13883	<i>Escherichia coli</i> ATCC 25922	<i>Salmonella typhi</i> ATCC 14028	<i>Bacillus subtilis</i> ATCC 6051	<i>Staphylococcus aureus</i> ATCC 25923	<i>Streptococcus pyogenes</i> ATCC 12346
1	2a	7.81	12.00	5.80	17.80	18.67	13.42
2	2b	22.11	20.15	24.19	26.09	24.10	27.99
3	2c	16.57	18.55		13.28	18.17	17.01
4	2d		4.00		10.00	7.80	
5	2e	7.10	5.00	6.89	5.77	13.62	13.00
6	2f	13.05	13.05	7.30		5.35	
7	2g	8.31	9.11	13.13	19.56	13.13	
8	2h	15.60	17.55	13.41		12.40	
9	2i	27.77	26.82	27.70	24.19	25.03	23.01
10	2j			3.99		9.11	
11	levofloxacin	32.07	30.11	29.01	35.10	28.05	31.11

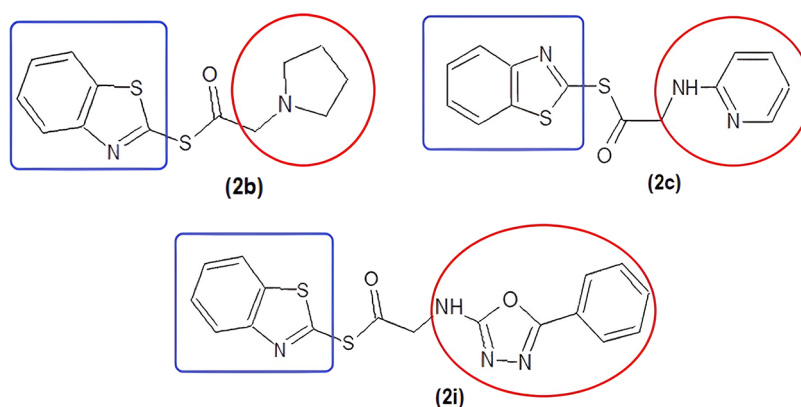
^aLevofloxacin (LF).

Figure 1. Structure–activity relationship of 2b, 2c, and 2i. The figure indicates benzothiazole moiety (blue square) linked with different heterocyclic amines (red circle) via the amide bond.

sulfur atom in the cyclic systems along with nitrogen further improved the therapeutic potential. As amide linkages and benzothiazole are considered as biological isosteres, the present study was designed to synthesize structural hybrids containing benzothiazole and different amines to explore their antibacterial potential. Since many of the existing antibiotics have lost their efficacy due to emerging resistance, our aim in the present study was to develop antibacterial lead molecules that can also target these resistance mechanisms, such as biofilm formation.

Keeping in view the above-mentioned facts and search for new potent antibacterial candidates, the present study was designed to synthesize new hybrid molecules containing benzothiazole linked with different aryl and heterocyclic amines and evaluate them for *in vitro* antibacterial potential, antibiofilm activity, and *in silico* mechanistic investigation.

2. RESULTS AND DISCUSSION

2.1. Synthesis and Characterization of 2-Mercapto-benzothiazole Acetamide Derivatives. In the present work, 2-mercaptobenzothiazole was reacted with chloroacetylchloride to yield its acetamide derivative as a key intermediate (1) in the first step, which in turn was treated with a series of different aryl/heterocyclic amines (a–j), leading to the formation of the target 2-mercaptobenzothiazole derivatives 2(a–j), as shown in Scheme 1. The structural details of the

synthesized compounds are presented in Table 1. The physical parameters of the synthesized compounds, including melting form, physical form, percentage (% age) yield, and R_f values along with molecular formula and molecular weights, were determined and are given in Table 6. All of the compounds were obtained as solids with sharp melting points. The progress of each reaction was monitored by TLC and the structural characterization was done by Fourier transform infrared (FTIR), ¹H NMR, and ¹³C NMR spectroscopic data. FTIR spectra showed prominent peaks for carbonyl stretchings at 1607–1684 cm^{–1}, confirming the formation of the desired compounds. Other important peaks included carbon–halogen stretchings in the range 810–718 cm^{–1}, C=C peaks at 1596–1460 cm^{–1}, and NH stretching peaks at higher frequencies in all compounds. In the ¹H NMR spectra of the synthesized compounds, all of the protons resonated in their respective regions. The characteristic singlet peak of the linker CH₂ was observed in the region 2.03–4.75 ppm, present in all derivatives and confirming the formation of the product, while aromatic protons of benzothiazole moiety resonated as multiplets at 7.25–7.87 ppm. In the case of the morpholine-containing compound 2a, two multiplets for morpholine protons were observed, while pyrrolidine hydrogens appeared as multiplets in the expected region. In case of ansidine-containing derivatives, methoxy protons resonated as singlets at 3.80 ppm. Similarly, for the benzylamine-containing

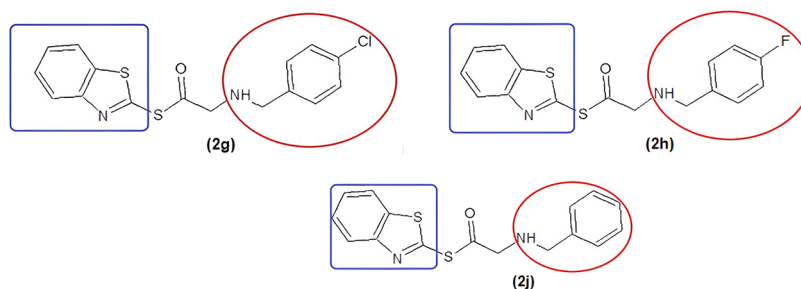


Figure 2. Structure–activity relationship of **2g**, **2h**, and **2j**. The figure indicates benzothiazole moiety (blue square) linked with different heterocyclic amines (red circle) via the amide bond.

Table 3. Minimum Inhibitory Concentration (MIC in $\mu\text{g}/100 \mu\text{L}$) of the Test Compounds

Sr. No.	codes		inhibition zone of bacterial growth (mm)					
			Gram (–) bacteria			Gram (+) bacteria		
			<i>K. pneumoniae</i> ATCC 13883	<i>E. coli</i> ATCC 25922	<i>S. typhi</i> ATCC 14028	<i>B. subtilis</i> ATCC 6051	<i>S. aureus</i> ATCC 25923	<i>S. pyogenes</i> ATCC 12346
1	2b	25 $\mu\text{g}/100 \mu\text{L}$	22.11	20.15	24.19	26.09	24.10	27.99
		50 $\mu\text{g}/100 \mu\text{L}$	36.21	35.12	37.01	36.03	35.91	38.11
		75 $\mu\text{g}/100 \mu\text{L}$	57.07	54.55	55.15	53.08	58.77	57.01
		MIC ($\mu\text{g}/100 \mu\text{L}$)	48.93	32.43	30.92	18.07	33.26	48.93
2	2i	25 $\mu\text{g}/100 \mu\text{L}$	27.77	26.82	27.70	24.19	25.03	23.01
		50 $\mu\text{g}/100 \mu\text{L}$	38.71	35.72	37.42	36.17	38.33	33.71
		75 $\mu\text{g}/100 \mu\text{L}$	52.06	50.14	56.77	57.12	58.07	51.13
		MIC ($\mu\text{g}/100 \mu\text{L}$)	48.85	30.54	27.82	23.94	31.70	48.85
3	LF	25 $\mu\text{g}/100 \mu\text{L}$	32.07	30.11	29.01	35.10	28.05	31.11
		50 $\mu\text{g}/100 \mu\text{L}$	39.77	40.32	41.22	39.77	40.23	43.71
		75 $\mu\text{g}/100 \mu\text{L}$	59.06	60.11	58.17	59.12	63.01	57.73
		MIC ($\mu\text{g}/100 \mu\text{L}$)	35.33	28.86	32.63	23.50	37.81	35.33

compounds (**2g**, **2h**, and **2j**), an extra singlet for two methylene protons was observed up-field. ^{13}C NMR was also performed, which further confirmed the synthesis of the target derivatives **2(a–j)**. The characteristic peak of the linker CH_2 carbon was noticed at 49.2–49.5 ppm in all derivatives. In addition, some characteristic peaks of 2-mercaptobenzothiazole were observed in the aromatic range of 121 ppm to 166 ppm, while acetamide carbonyl carbon resonated downfield at 166–168 ppm in all of the final compounds **2(a–j)**. In case of **2a** and **2b**, the CH_2 of morpholine and pyrrolidine moiety were observed up-field in the range of 3.56–3.65 and 2.03–3.03 ppm, respectively.

2.2. Antimicrobial and Antibiofilm Activity. The 2-mercaptobenzothiazole moiety has been previously reported to possess strong antibacterial activity and referred to as a good antimicrobial agent.²⁴ Based on its antibacterial potential, it was linked with different amines with the aim of enhancing its potency. All of the synthesized compounds **2(a–j)** were screened for their antibacterial activity against both Gram-positive and Gram-negative species using the agar well diffusion method. All of the synthesized derivatives exhibited moderate to good antibacterial activity with few exceptions where a part of the activity might be due to the 2-mercaptobenzothiazole moiety itself.²⁵ The antibacterial activities of all of the synthetic hybrids are summarized in Table 2. Among these, **2b** and **2c** showed promising activity against all strains, while **2i** showed maximum antibacterial activity against all bacterial strains.

It was observed that the structure of potent derivatives contained benzothiazole linked through amide bonds to different heterocyclic amines, e.g., with oxadiazole moiety in

the case of compound **2i**, while the other two active compounds, **2b** and **2c**, also contained heterocyclic amine moieties, pyrrolidine and pyridine moieties, respectively (Figure 1). This clearly indicated the better antimicrobial potential of heterocyclic amines as compared to simple substituted anilines or benzyl amines.

Benzylamine containing derivatives **2g**, **2h**, and **2j** showed moderate activity against both Gram-positive and Gram-negative bacteria. Moreover, **2g** exhibited maximum activity against the Gram-negative specie *B. subtilis*, while **2h** was found to be more selective for the Gram-positive species. The activity of these derivatives may be attributed to the halogens present in these compounds, while **2j** having no halogen substitution was almost inactive (Figure 2). In general, the derivatives with more electron-withdrawing groups on the amine moiety were found to be more active as compared to the electron-donating groups bearing amine moieties, as is evident from the least zone of inhibitions shown by the anisidine-containing derivatives **2d**, **2e**, and **2f**.

As compounds **2b** and **2i** showed good antibacterial activity, comparable with standard levofloxacin, their activities were further observed at different concentrations (25, 50, 75 $\mu\text{g}/100 \mu\text{L}$) and their minimum inhibitory concentrations (MIC) were calculated against the same bacterial strains. Both the compounds **2b** and **2i** exhibited MIC values close to the positive control, especially against *E. coli*, *S. typhi*, *S. aureus*, and *B. subtilis*. In the case of *B. subtilis*, the MIC of **2b** was even lower than that of the standard drug levofloxacin, and the MIC of **2i** was equal to that of positive control. Similarly, in the case of *S. typhi* and *S. aureus*, both the synthesized compounds **2b** and **2i** exhibited lower MIC as compared to the standard drug.

This significant activity of compounds **2b** and **2i** might be due to the presence of specific heterocyclic amine moieties, i.e., pyrrolidine ring in the case of compound **2b** and amino oxadiazole ring in the case of compound **2i**. The antimicrobial activities in terms of MIC for the standard and compounds **2b** and **2i** have been summarized in Table 3.

Biofilm confers several advantages to the pathogens, notably during the colonization process of medical devices and/or body organs. In addition, sessile bacteria have a high tolerance to exogenous stress, including anti-infectious agents. Biofilms are highly competitive communities and some microorganisms exhibit antibiofilm capacities such as bacterial growth inhibition, exclusion, or competition, which enable them to acquire advantages and become dominant. The deciphering and control of antibiofilm properties represent future challenges in human infection control.^{26,27} In the current study, synthesized compounds **2i**, **2b**, and **2c** were selected on the basis of their good antibacterial activities and were evaluated for antibiofilm activity against biofilm-forming bacteria *S. aureus* and *K. pneumoniae* in a dose-dependent manner at two different concentrations, i.e., 50 $\mu\text{g}/100 \mu\text{L}$ and 100 $\mu\text{g}/100 \mu\text{L}$, respectively. The antibiofilm activity was expressed as the percent inhibition of the test samples using cefadroxil as positive control and DMSO as negative control. It was observed that compounds **2i**, **2b**, and **2c** exhibited significant antibiofilm activity, even better than positive control, especially at a higher concentration of 100 $\mu\text{g}/100 \mu\text{L}$. Treatment of *S. aureus* and *K. pneumoniae* with **2i** (100 $\mu\text{g}/100 \mu\text{L}$) reduced the biofilm formation by 82 and 85%, respectively, as compared to the standard drug, which inhibited biofilm formation by 72 and 83%. Similarly, **2b** and **2c** also reduced the biofilm formation by >80%, which clearly indicated the greater antibiofilm potential of our synthesized compounds as compared to the positive control. Again, the excellent antibiofilm potential of these compounds can be attributed to the presence of bioactive heterocyclic scaffolds. In addition to benzothiazole moiety, the pyrrolidine ring in compound **2b**, pyridine ring in compound **2c**, and amino oxadiazole in the case of compound **2i** rendered better antibacterial potential as well as antibiofilm activity to these compounds. The results of the present research confirm the efficacy of our synthesized hybrid compounds against biofilms produced by the Gram-negative bacterium, *K. pneumoniae*, and the Gram-positive bacterium, *S. aureus*. The antibiofilm activities of compounds **2i**, **2b**, and **2c** have been shown in Table 4.

Table 4. Antibiofilm Activity Table for Compounds **2i, **2b**, and **2c**^a**

testing samples	% inhibition (100 $\mu\text{g}/100 \mu\text{L}$)		% inhibition (50 $\mu\text{g}/100 \mu\text{L}$)	
	<i>Staphylococcus aureus</i>	<i>Klebsiella pneumoniae</i>	<i>Staphylococcus aureus</i>	<i>Klebsiella pneumoniae</i>
2i	82.68	85.10	70.83	72.82
2b	80.99	85.92	60.85	73.28
2c	83.48	80.65	64.58	70.38
positive control	72.23	83.83	72.03	80.45
negative control	~0	~0	5.3	~0

^aPercent inhibition of test samples in the antibiofilm activity against *S. aureus* and *K. pneumoniae*. Positive control (antibiotic) was cefadroxil (5 $\mu\text{g}/5 \mu\text{L}$), whereas negative control was DMSO.

2.3. In Silico Docking Analysis. The docking studies were done in an effort to predict the mechanisms of antibacterial activity of the test molecules.²⁸ Based on the results of the activities, compounds that had good activity were screened for potential targets by LigTmap server, which showed that these would have a high affinity for bacterial kinases and gyrases, on the basis of which docking studies were performed. The binding affinities of the synthesized ligands and the standard drug levofloxacin have been shown in Table 5. For this

Table 5. Docking Results of Compounds **2a–j^a**

ligand	bacterial kinases		bacterial gyrases	
	1OS1	4X8L	4DUH	4WUB
2a	−8.4	−8.3	−7.2	−8.2
2b	−7.3	−7.9	−7.1	−7.6
2c	−8.9	−8.6	−7.3	−8.1
2d	−8.8	−9.0	−7.7	−8.4
2e	−8.9	−8.8	−7.6	−8.5
2f	−8.3	−8.9	−7.6	−8.3
2g	−9.4	−8.8	−7.8	−8.2
2h	−8.2	−8.8	−7.8	−8.1
2i	−10.7	−10.5	−8.9	−9.5
2j	−9.1	−8.6	−7.6	−8.1
levofloxacin	−7.8	−9.1	−8.2	−8.0

^aBinding affinities are given in kcal/mol.

purpose, protein structures of bacterial kinases (1OS1, 4X8L) and bacterial gyrases (4DUH, 4WUB) were downloaded from the protein data bank. The structures of these proteins have been shown in Figure 3. 1OS1 represents the structure of phosphoenolpyruvate carboxykinase, while 4X8L expresses the crystal structure of *E. coli* adenylate kinase P177A mutant. Also, 4DUH represents the crystal structure of the protein 24 kDa domain of *E. coli* DNA gyrase B, while 4WUB represents another DNA gyrase (N-terminal 43 kDa fragment of the *E. coli* DNA gyrase B subunit grown from 100 mM KCl condition). Interestingly, the synthetic molecule **2i** exhibited the lowest binding energy against protein kinases (1OS1, 4X8L) and DNA gyrases (4DUH, 4WUB), which was comparable to the clinical drug levofloxacin. In case of 1OS1, **2i** exhibited stable hydrogen bonds with THR255, GLY253, GLY251, SER2590, and ARG233, while levofloxacin had hydrogen bond interaction with LYS288. In case of another bacterial kinase, 4X8L, hydrogen bonds were observed between the ligand **2i** and ARG36 and ARG156, while levofloxacin exhibited multiple hydrogen bond interactions with GLY14, LYS13, ARG123, GLY10, and ARG11. As for bacterial DNA gyrases 4DUH, **2i** showed hydrogen bond interactions with LYS103, ALA100, and ASN46, while in the case of levofloxacin, hydrogen bond interactions were observed with ASN46, ARG76, GLY77, and GLY101. In the case of the bacterial DNA gyrase 4WUB, hydrogen bonds were observed with GLU50, LEU115, and THR165, while for levofloxacin such interactions involved TYR109 during *in silico* analysis. Strikingly, molecule **2i** and levofloxacin were docked in the same hydrophobic binding pocket of the protein kinases and DNA gyrases (Figures 4C–7C). Indeed, the results of *in vitro* analysis were in good agreement with the docking studies (Table 5, Figures 4–7). The mechanism of action of levofloxacin involves the inhibition of bacterial deoxyribonucleic acid (DNA) gyrase, a type II topoisomerase that makes it active against a broad range of bacterial species. Along the

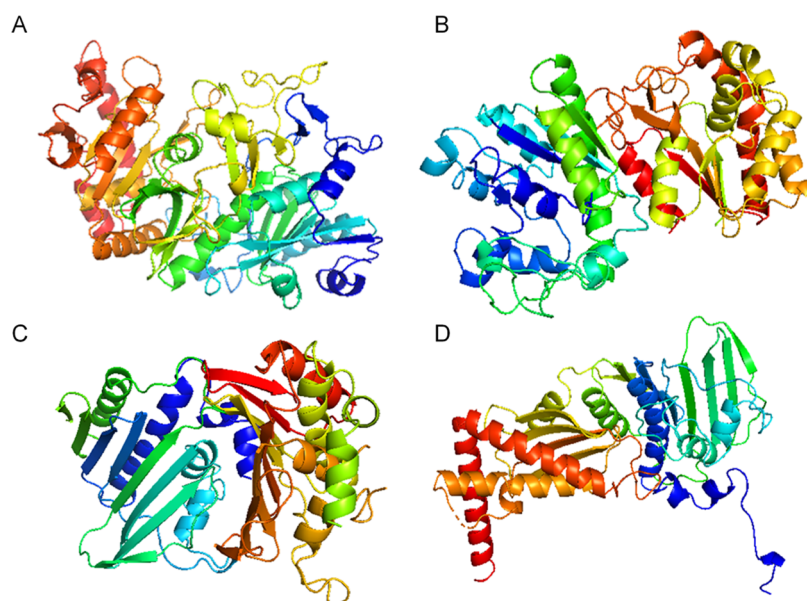


Figure 3. Structure of the bacterial kinases and DNA gyrases used in docking analysis. The structures were downloaded from the protein data bank. (A) 1OS1, (B) 4X8L, (C) 4DUH, (D) 4WUB. 1OS1, phosphoenolpyruvate carboxykinase; 4X8L, *E. coli* adenylate kinase P177A mutant; 4DUH, 24 kDa domain of *E. coli* DNA gyrase B; 4WUB, N-terminal 43 kDa fragment of the *E. coli* DNA gyrase B subunit grown from 100 mM KCl condition.

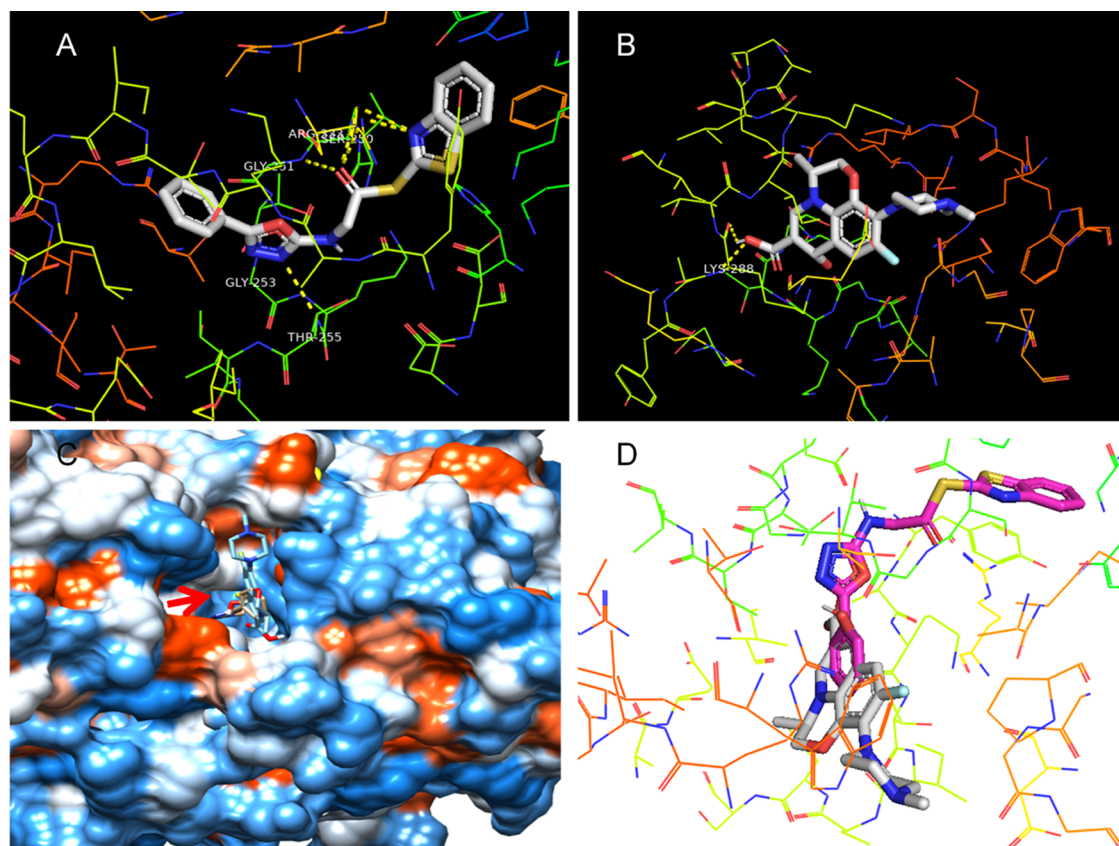


Figure 4. Binding mode of ligand **2i** and levofloxacin with 1OS1. (A) Docked complex of **2i** with 1OS1. (B) Docked complex of levofloxacin with 1OS1. (C) **2i** and levofloxacin are docked in the same hydrophobic binding pocket as visualized by the UCSF chimera. An enlarged view of the same has been shown in (D) as visualized by PyMOL, with **2i** in magenta color while levofloxacin has been colored gray. The dotted yellow lines indicate hydrogen bond interactions between the molecules and labeled residues. 1OS1, phosphoenolpyruvate carboxykinase.

same lines, *in silico* analysis indicated that **2i** could inhibit bacterial DNA gyrases as well as bacterial kinases, which could be responsible for the remarkable *in vitro* activities. However,

future studies are desirable to further confirm these activities *in vivo* and in cell culture base assays.d

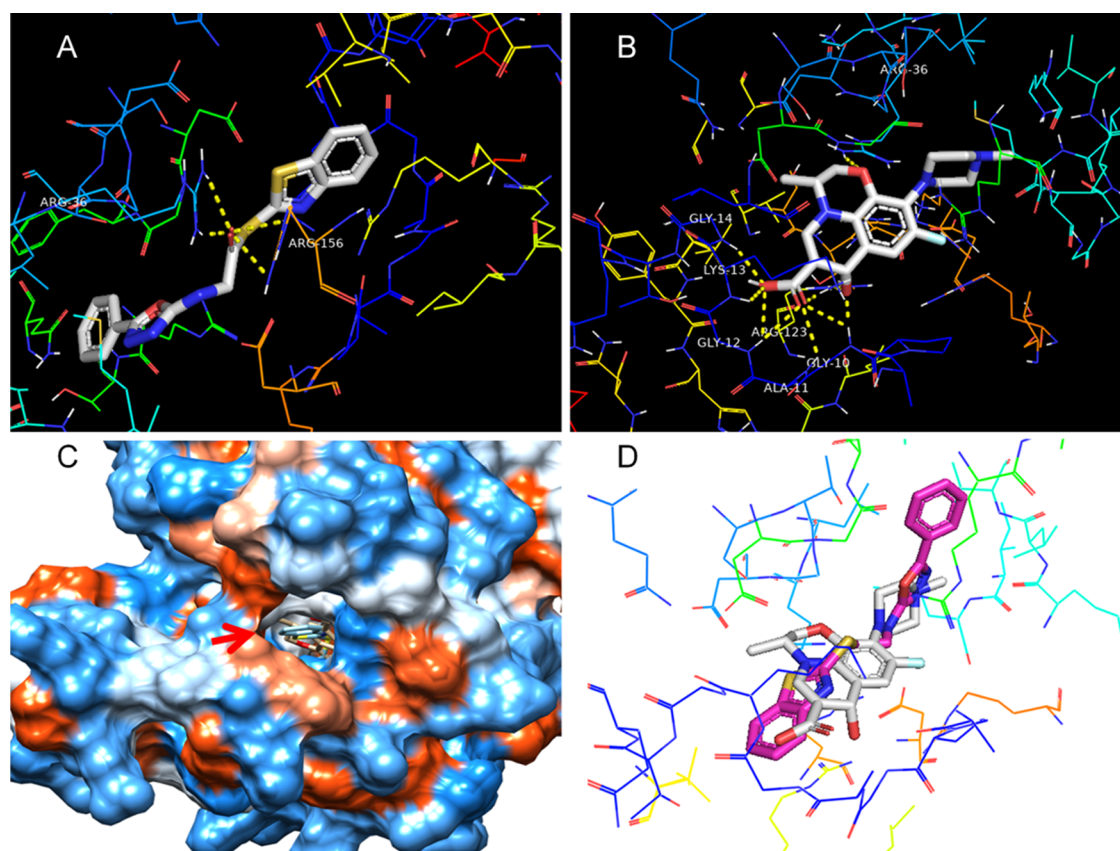


Figure 5. Binding mode of ligand **2i** and levofloxacin with 4X8L. (A) Docked complex of **2i** with 4X8L. (B) Docked complex of levofloxacin with 4X8L. (C) **2i** and levofloxacin were docked in the same hydrophobic binding pocket as visualized by UCSF chimera. An enlarged view of the same has been shown in (D) as visualized by PyMOL, with **2i** in magenta color while levofloxacin has been colored gray. The dotted yellow lines indicate hydrogen bond interactions between the molecules and labeled residues. 4X8L, *E. coli* adenylate kinase P177A mutant.

3. CONCLUSIONS

The present study resulted in the successful synthesis of ten new 2-mercaptobenzothiazole acetamide derivatives **2(a–j)** in good yields. All of the derivatives were characterized by FTIR, ^1H NMR, and ^{13}C NMR spectral analysis. Further, these molecules were screened for their antimicrobial potential against different Gram-positive and Gram-negative strains. Among the synthesized derivatives, compounds **2b**, **2c**, and **2i** exhibited significant antibacterial potential at different concentrations. The MIC values for most active compounds were found to be comparable to that of the standard, levofloxacin. Moreover, Gram-positive strains were found to be more susceptible to the antibacterial action of active compounds, while such promising activity of compounds **2b** and **2i** might be due to the specific heterocyclic rings system: pyrrolidine ring in compound **2b** and amino oxadiazole ring in compound **2i**. Compounds **2i**, **2b**, and **2c** were further investigated for their antibiofilm activity at two different concentrations: 50 $\mu\text{g}/100\ \mu\text{L}$ and 100 $\mu\text{g}/100\ \mu\text{L}$. It was observed that these derivatives showed excellent antibiofilm activity, even better than positive control, which may well be responsible for the enhanced antibacterial potential in the case of resistant strains. The presence of heterocyclic moieties in **2b**, **2c**, and **2i** clearly suggested their potential to design better antibacterial agents. Docking studies were performed to predict the mechanisms of antibacterial activity. Amazingly, the molecule **2i** shared the same hydrophobic pockets as those of levofloxacin in case of bacterial kinases and DNA gyrases. In

addition, **2i** exhibited satisfactory antibiofilm activity in comparison with the standard. In conclusion, the synthetic compounds **2b** and **2i** possess significant antibacterial and antibiofilm activity and may serve as promising lead molecules for further optimization in the journey to discover potent antibacterial agents.

4. EXPERIMENTAL SECTION

4.1. General Details. Analytical grade chemicals were used in the present work, which were purchased from Sigma Aldrich, Fluka, and Merck. The melting point (mp) was determined, employing a G-k [SANYO] model MPD BM 3.5 digital device. The progression of the reaction process was checked by thin-layer chromatography (TLC) HF254-coated plates (Merck). ^1H NMR spectra were measured using a (Bruker) AM300 photometer in dimethyl sulfoxide (DMSO) at 300 megahertz (MHz) using standard tetra methyl silane (TMS) as an internal standard. The unit of chemical shift (CS) (δ) was ppm. Attainment of MS spectra was done *via* a 6890 N instrument (Agilent Technologies) equipped with a 5973-mass detector. FTIR analysis was done with the aid of a Thermo Scientific (NICOLET IS10) spectrophotometer (potassium bromide; KBr), (ν_{max} in cm^{-1}) and an ANALYST 2000CHNS analyzer (Perkin Elmer) was used for analysis of the elements present. The physical data of the synthesized compounds have been summarized in Table 6

4.2. General Synthesis Procedure for 5-(1,3-Benzothiazol-2-yl) Chloro-ethane-thionate (1). 2-Mercaptoben-

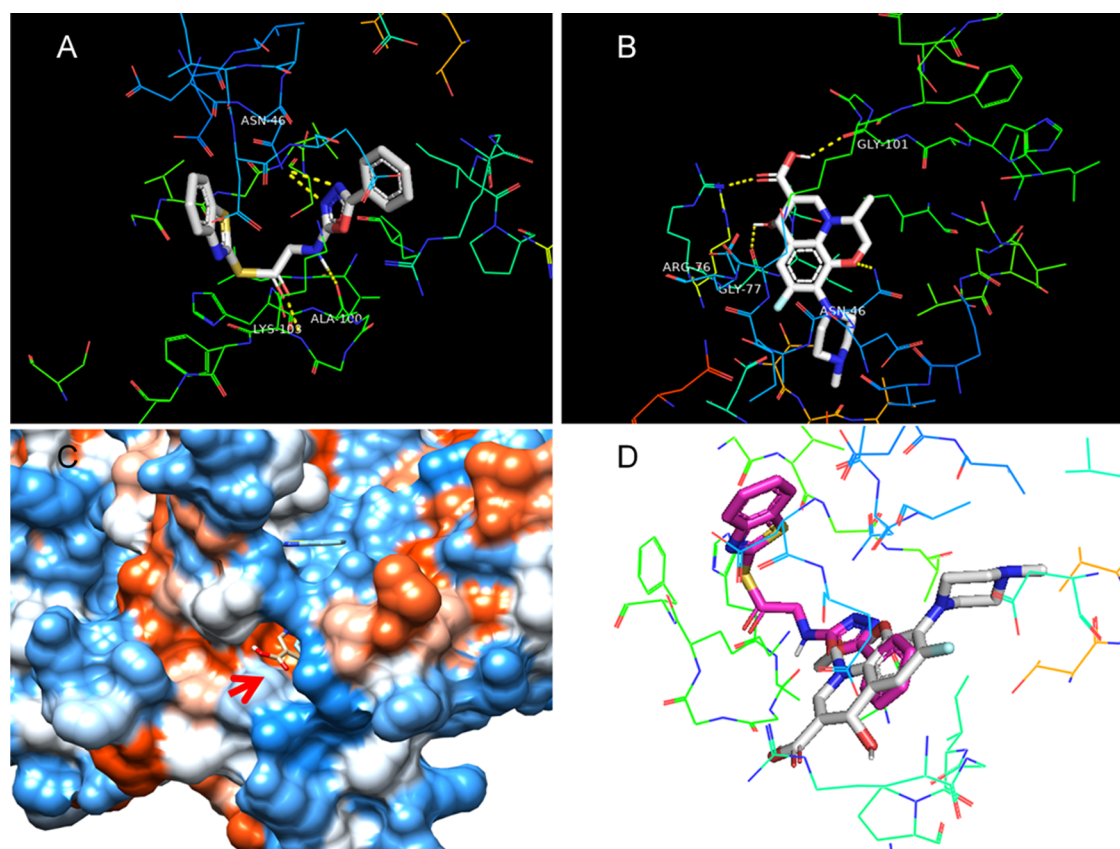


Figure 6. Binding mode of ligand **2i** and levofloxacin with 4DUH. (A) Docked complex of **2i** with 4DUH. (B) Docked complex of levofloxacin with 4DUH. (C) **2i** and levofloxacin were docked in the same hydrophobic binding pocket as visualized by UCSF chimera. An enlarged view of the same has been shown in (D) as visualized by PyMOL, with **2i** in magenta color while levofloxacin has been colored gray. The dotted yellow lines indicate hydrogen bond interactions between the molecules and labeled residues. 4DUH, 24 kDa domain of *E. coli* DNA gyrase B.

zathiazole (0.05 mol) was dissolved in dry dichloromethane (30 mL) in the presence of anhydrous K_2CO_3 (0.05 mol) and chloroacetylchloride (0.05 mol) was added dropwise, while keeping the mixture in an ice bath for 15 min at controlled temperature (0–5 °C). After the complete addition, the mixture was stirred at room temperature for 24 h and TLC was used to observe the progression of the reaction (ethyl acetate:petroleum 3:2). The mixture was left at 25 °C for 24 h and then transferred to crushed ice. The residual solid was filtered by removing the solvent under vacuum to dryness. The ethanol–water mixture was used for recrystallization of the dried solid.²⁹

4.2.1. General Procedure for the Synthesis of 2-Mercaptobenzothiazole Acetamide Derivatives (2a–j). A reported procedure was used with minor modifications.³⁰ Equimolar quantities (0.05 mol) of compound **1** and anhydrous potassium carbonate in DMF were stirred at room temperature for 2 h followed by the dropwise addition of 0.05 mol of compounds (a–j) in DMF. The mixture was refluxed further with stirring for 12 h. TLC (ethyl acetate/pet. ether, 3:2) was used to verify the completion of the reaction. The solvent was evaporated and the residue extracted with ethyl acetate, evaporated, and the solid obtained was dried. The codes, substrate, product, and yield of the synthesized analogues have been indicated in Table 1.

4.2.2. Synthesis of S-1,3-Benzothiazol-2-yl morpholine-4-yl ethanethionate (2a). Yellow crystalline solid, m.p. 119 °C; yield (88%), pet. ether/ethyl acetate (2:3). IR (KBr, cm^{-1}): 2919 ($-CH_2$), 1684 ($C=O$), 1189 ($C-N$), 1554 ($C=N$),

1415 ($C=C$), 795 ($C-S$). 1H NMR: δ 2.56–3.43 (m, 4H, Morpholine-H), 3.56 (s, 2H, $-CH_2$), 3.60–3.65 (m, 4H, Morpholine-H), 7.26–7.84 (m, 4H, Ar-H). ^{13}C NMR (DMSO- d_6 , 300 MHz, δ ppm): 49.2 ($-CH_2$), Morpholine-C {53.7 (2C, s), 66.3 (2C, s)}, Ar-C {121.8, 122.4, 124.9, 126.4, 135.9, 152.8, 165.7}, 193.3 ($C=O$). MS m/z (%): 294.04, Anal. Calcd for $C_{13}H_{14}N_2O_2S_2$ (294.39): C, 53.04; N, 9.52; H, 4.79; O, 10.87; S, 21.78%. Found: C, 52.04; N, 9.02; H, 4.19; O, 10.07; S, 20.72%.

4.2.3. Synthesis of S-1,3-Benzothiazol-2-yl pyrrolidin-1-yl ethanethionate (2b). Pale white solid with m.p. 155 °C; yield (83%), pet. ether/ethyl acetate (2:3). IR (KBr, cm^{-1}): 3148 ($-CH_2$), 1657 ($C=O$), 1095 ($C-N$), 1543 ($C=N$), 1515 ($C=C$), 1250 ($C-O$), 1349 ($C=S$), 845 ($C-S$). 1H NMR: δ 1.56–2.25 (m, 4H, Pyrrolidine-H), 2.56–3.43 (m, 4H, Pyrrolidine-H), 3.54 (s, 2H, $-CH_2$), 7.23–7.82 (m, 4H, Ar-H). ^{13}C NMR (DMSO- d_6 , 300 MHz, δ ppm): 49.2 ($-CH_2$), Pyrrolidine-C {23.4, 53.7}, Ar-C {121.8, 122.4, 124.9, 126.4, 135.9, 152.8, 165.7}, 193.3 ($C=O$). MS m/z (%): 278.05, Anal. Calcd for $C_{13}H_{14}N_2OS_2$ (278.4): C, 56.09; N, 10.06; H, 5.07; O, 5.75; S, 23.04%. Found: C, 56.04; N, 9.12; H, 4.99; O, 5.07; S, 22.92%.

4.2.4. Synthesis of S-1,3-Benzothiazol-2-yl (pyridin-2-ylamino)ethanethionate (2c). Light orange crystalline solid with m.p. 150 °C; yield (77%), pet. ether/ethyl acetate (2:3). IR (KBr, cm^{-1}): 3404 (NH), 2987 ($-CH_2$), 1668 ($C=O$), 1033 ($C-N$), 1502 ($C=C$), 1395 ($C=S$), 833 ($C-S$). 1H NMR: δ 3.63 (s, 2H, $-CH_2$), 6.97–6.99 (dd, 1H, $J = 6.7$ Hz, Pyridyl-H), 7.13–7.44 (dd, 4H, $J = 7.1$ Hz, Ar-H), 7.52–7.82

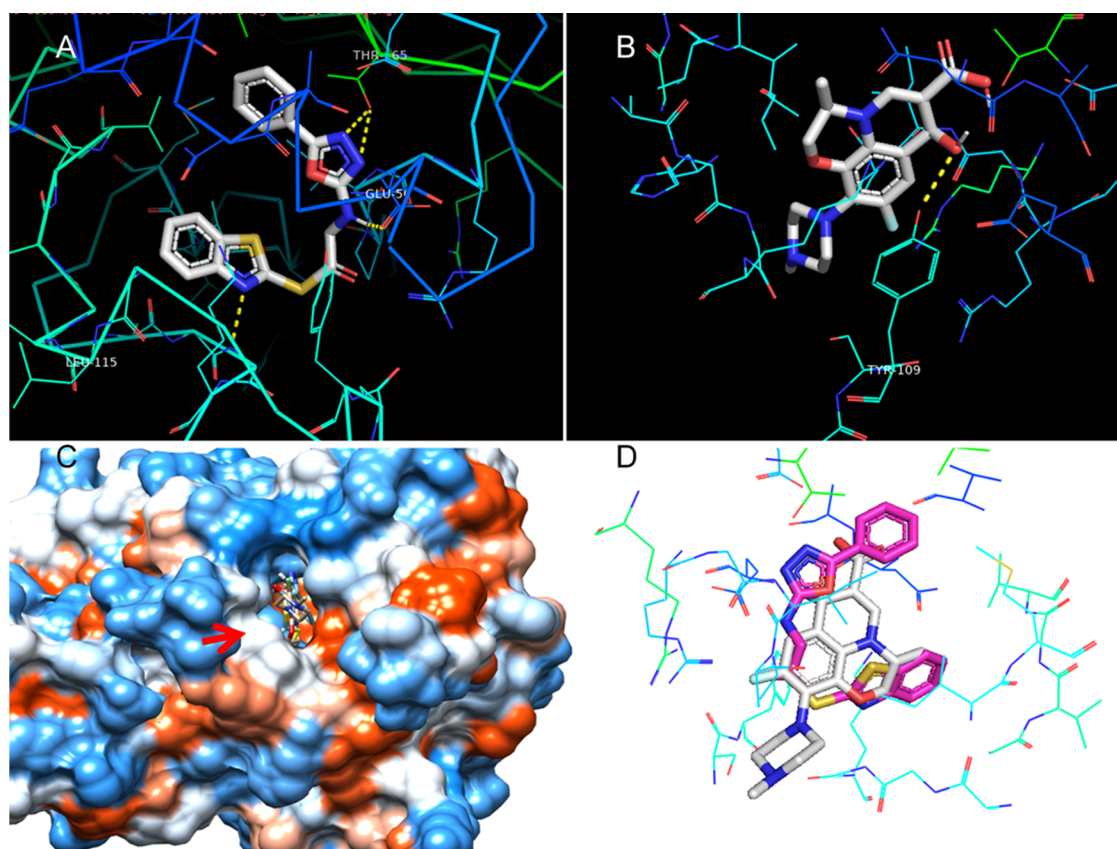


Figure 7. Binding mode of ligand **2i** and levofloxacin with 4WUB. (A) Docked complex of **2i** with 4WUB. (B) Docked complex of levofloxacin with 4WUB. (C) **2i** and levofloxacin were docked in the same hydrophobic binding pocket as visualized by UCSF chimera. An enlarged view of the same has been shown in (D) as visualized by PyMOL, with **2i** in magenta color while levofloxacin has been colored gray. The dotted yellow lines indicate hydrogen bond interactions between the molecules and labeled residues. 4WUB, N-terminal 43 kDa fragment of the *E. coli* DNA gyrase B subunit grown from 100 mM KCl condition.

Table 6. Physical Data of the Synthesized Compounds (2a–j)^a

compounds	mol. formula	mol. weight (g)	mp (°C)	physical form	% yield	R _f value
2a	C ₁₃ H ₁₄ N ₂ O ₂ S ₂	294.39	119	solid	88	0.86
2b	C ₁₃ H ₁₄ N ₂ OS ₂	278.4	155	solid	83	0.70
2c	C ₁₄ H ₁₁ N ₃ OS ₂	301.38	150	solid	77	0.81
2d	C ₁₆ H ₁₄ O ₂ N ₂ S ₂	330.42	220	solid	75	0.85
2e	C ₁₆ H ₁₄ O ₂ N ₂ S ₂	330.42	95	solid	81	0.77
2f	C ₁₆ H ₁₄ O ₂ N ₂ S ₂	330.42	145	solid	69	0.67
2g	C ₁₆ H ₁₃ N ₂ OClS ₂	348.8	255	solid	83	0.83
2h	C ₁₆ H ₁₃ N ₂ FOS ₂	332.4	190	solid	75	0.74
2i	C ₁₇ H ₁₂ N ₄ O ₂ S ₂	368.4	193	solid	70	0.68
2j	C ₁₆ H ₁₄ N ₂ OS ₂	314.4	125	solid	76	0.76

^a(Pet. ether/ethyl acetate, 2:3), (HF-254)- silica.

(m, 2H, Pyridyl-H), 8.22–8.28 (dd, 1H, *J* = 8.1 Hz, Pyridyl-H), 9.62 (s, 1H, N-H). ¹³C NMR (DMSO-*d*₆, 300 MHz, δ ppm): 49.2 (-CH₂), Pyridyl-C {107.6, 118.9, 137.7, 148.0, 158.5}, Ar-C {121.8, 122.4, 124.9, 126.4, 135.9, 152.8, 165.7}, 193.3 (C=O). MS *m/z* (%): 301.03, Anal. Calcd for C₁₄H₁₁N₃OS₂ (301.38): C, 55.78; N, 13.94; H, 3.68; O, 5.31; S, 21.28%. Found: C, 53.04; N, 12.12; H, 3.09; O, 4.07; S, 19.92%.

4.2.5. Synthesis of *S*-1,3-Benzo-thiazol-2-yl [(3-methoxyphenyl)amino]ethanethionate (2d**).** Pale yellow crystalline solid with m.p. 220 °C; yield (75%), pet. ether/ethyl acetate (2:3). IR (KBr, cm⁻¹): 3294 (NH), 2935 (-CH₂), 1642 (C=O), 1025 (C–N), 1226 (C–O), 1552 (C=N),

1394 (C=C), 1162 (C=S), 830 (C–S). ¹H NMR: δ 2.83 (s, 2H, -CH₂), 4.12 (s, 3H, -OCH₃), 6.52–6.59 (d, 1H, Ar-H), 6.70–6.76 (d, 1H, Ar-H), 6.82–6.96 (d, 1H, Ar-H), 7.01–7.13 (dd, 1H, *J* = 7.1 Hz, Ar-H), 7.22–7.29 (m, 4H, Ar-H), 8.17 (s, 1H, N-H). ¹³C NMR (DMSO-*d*₆, 300 MHz, δ ppm): 49.2 (-CH₂), 55.4 (OCH₃), Ar-C {21.8, 22.4, 35.9, 52.8, 65.7, 106.2, 108.2, 119.1, 124.9, 126.4, 130.4, 144.3, 160.2}, 193.3 (C=O). MS *m/z* (%): 330.04, Anal. Calcd for C₁₆H₁₄O₂N₂S₂ (330.42): C, 58.16; N, 8.48; H, 4.27; O, 9.68; S, 19.41%. Found: C, 57.04; N, 8.12; H, 4.09; O, 8.07; S, 17.92%.

4.2.6. Synthesis of *S*-1,3-Benzo-thiazol-2-yl [(4-methoxyphenyl)amino]ethanethionate (2e**).** Amorphous white solid with m.p. 95 °C; yield (81%), pet. ether/ethyl

acetate (2:3). IR (KBr, cm^{-1}): 3422 (NH), 2986 ($-\text{CH}_2$), 1636 ($\text{C}=\text{O}$), 1030 ($\text{C}-\text{N}$), 1239 ($\text{C}-\text{O}$), 1596 ($\text{C}=\text{N}$), 1442 ($\text{C}=\text{C}$), 1158 ($\text{C}=\text{S}$), 845 ($\text{C}-\text{S}$). ^1H NMR: δ 2.77 (s, 2H, $-\text{CH}_2$), 4.65 (s, 3H, $-\text{OCH}_3$), 6.84–6.89 (dd, 2H, $J = 6.7$ Hz, Ar-H), 6.90–6.92 (dd, 2H, $J = 6.8$ Hz, Ar-H), 7.28–7.39 (m, 4H, Ar-H), 8.92 (s, 1H, N-H). ^{13}C NMR (DMSO- d_6 , 300 MHz, δ ppm): 49.2 ($-\text{CH}_2$), 55.4 (OCH_3), Ar-C {65.9, 121.8, 122.8, 123.2, 124.9, 126.4, 135.9, 152.8, 166.8}, 193.3 ($\text{C}=\text{O}$). MS m/z (%): 330.04, Anal. Calcd for $\text{C}_{16}\text{H}_{14}\text{O}_2\text{N}_2\text{S}_2$ (330.42): C, 58.16; N, 8.48; H, 4.27; O, 9.68; S, 19.41%. Found: C, 57.04; N, 8.12; H, 4.09; O, 8.07; S, 17.92%.

4.2.7. Synthesis of S-1,3-Benzo-thiazol-2-yl [(2-methoxyphenyl)amino]ethanethionate (2f). White amorphous solid with m.p. 145 °C; yield (69%), pet. ether/ethyl acetate (2:3). IR (KBr, cm^{-1}): 3464 (NH), 2973 ($-\text{CH}_2$), 1625 ($\text{C}=\text{O}$), 1027 ($\text{C}-\text{N}$), 1247 ($\text{C}-\text{O}$), 1567 ($\text{C}=\text{N}$), 1496 ($\text{C}=\text{C}$), 1344 ($\text{C}=\text{S}$), 849 ($\text{C}-\text{S}$). ^1H NMR: δ 3.56 (2H, s), 2.94 (s, 2H, $-\text{CH}_2$), 4.89 (s, 3H, $-\text{OCH}_3$), 6.80–6.97 (m, 4H, Ar-H), 7.30–7.92 (m, 4H, Ar-H), 8.70 (s, 1H, N-H). ^{13}C NMR (DMSO- d_6 , 300 MHz, δ ppm): 49.2 ($-\text{CH}_2$), 55.9 (OCH_3), Ar-C {70.9, 55.4, 108.7, 110.2, 120.8, 124.2, 125.1, 127.4, 134.9, 147.6, 154.8, 164.7}, 195.3 ($\text{C}=\text{O}$). MS m/z (%): 330.04, Anal. Calcd for $\text{C}_{16}\text{H}_{14}\text{O}_2\text{N}_2\text{S}_2$ (330.42): C, 58.16; N, 8.48; H, 4.27; O, 9.68; S, 19.41%. Found: C, 57.04; N, 8.12; H, 4.09; O, 8.07; S, 17.92%.

4.2.8. Synthesis of S-1,3-Benzo-thiazol-2-yl phenoxyethanethionate (2g). Creamy amorphous white solid with m.p. 225 °C; yield (87%), pet. ether/ethyl acetate (2:3). IR (KBr, cm^{-1}): 2926 ($-\text{CH}_2$), 1650 ($\text{C}=\text{O}$), 1168 ($\text{C}-\text{N}$), 1388 ($\text{C}-\text{O}$), 1599 ($\text{C}=\text{N}$), 1468 ($\text{C}=\text{C}$), 1388 ($\text{C}=\text{S}$), 805 ($\text{C}-\text{S}$). ^1H NMR: δ 3.70 (s, 2H, $-\text{CH}_2$), 3.89 (s, 2H, $-\text{CH}_2$), 7.20–7.27 (dd, 2H, $J = 7.1$ Hz, Ar-H), 7.29–7.32 (dd, 2H, $J = 7.3$ Hz, Ar-H), 7.40–7.89 (m, 4H, Ar-H), 9.20 (s, 1H, N-H). ^{13}C NMR (DMSO- d_6 , 300 MHz, δ ppm): 49.2 ($-\text{CH}_2$), 53.5 ($-\text{CH}_2$), Ar-C {65.5, 114.8, 122.4, 123.5, 128.6, 129.6, 135.9, 144.7, 153.8, 164.7}, 194.3 ($\text{C}=\text{O}$). MS m/z (%): 301.02, Anal. Calcd for $\text{C}_{15}\text{H}_{11}\text{O}_2\text{N}_2\text{S}_2$ (301.4): C, 59.78; N, 4.65; H, 3.68; O, 10.68; S, 21.28%. Found: C, 59.04; N, 4.65; H, 3.09; O, 9.97; S, 19.92%.

4.2.9. Synthesis of S-1,3-Benzothiazol-2-yl [(4-fluorobenzyl)amino]ethanethionate (2h). Yellow crystalline solid with m.p. 190 °C; yield (75%), pet. ether/ethyl acetate (2:3). IR (KBr, cm^{-1}): 3349 (NH), 2945 (CH_2), 1639 ($\text{C}=\text{O}$), 1168 ($\text{C}-\text{N}$), 1475 ($\text{C}=\text{C}$) 828 ($\text{C}-\text{S}$), 1289 ($\text{C}=\text{S}$), 1532 ($\text{C}=\text{N}$), 1394 ($\text{C}-\text{O}$), 800 ($\text{C}-\text{F}$). ^1H NMR: δ 3.69 (s, 2H, $-\text{CH}_2$), 3.86 (s, 2H, $-\text{CH}_2$), 6.89–6.99 (dd, 2H, $J = 6.6$ Hz, Ar-H), 7.01–7.15 (dd, 2H, $J = 7.1$ Hz, Ar-H), 7.26–7.89 (m, 4H, Ar-H), 9.01 (s, 1H, N-H). ^{13}C NMR (DMSO- d_6 , 300 MHz, δ ppm): 49.05 ($-\text{CH}_2$), 54.2 ($-\text{CH}_2$), Ar-C {66.8, 115.0, 121.8, 122.5, 123.4, 126.5, 129.3, 135.7, 139.05, 152.8, 163.3}, 192.3 ($\text{C}=\text{O}$). MS m/z (%): 332.04, Anal. Calcd for $\text{C}_{16}\text{H}_{13}\text{N}_2\text{FO}$ (332.4): C, 57.81; N, 8.43; F, 5.72; H, 3.94; O, 4.81; S, 19.29%. Found: C, 54.08; N, 3.02; Cl, 10.06; H, 3.16; O, 4.49; S, 18.11%.

4.2.10. Synthesis of S-1,3-Benzo-thiazol-2-yl[(5-phenyl-1,3,4-oxadiazol-2-yl)amino]ethanethionate (2i). White crystalline solid, with m.p. 193 °C; yield (70%), pet. ether/ethyl acetate (2:3). IR (KBr, cm^{-1}): 3415 (NH), 2912 (CH_2), 1628 ($\text{C}=\text{O}$), 1175 ($\text{C}-\text{N}$), 1460 ($\text{C}=\text{C}$) 869 ($\text{C}-\text{S}$), 1212 ($\text{C}=\text{S}$), 1540 ($\text{C}=\text{N}$), 1376 ($\text{C}-\text{O}$), 718 ($\text{C}-\text{F}$). ^1H NMR: δ 4.01 (s, 2H, $-\text{CH}_2$), 6.68–6.70 (m, 1H, Ar-H), 6.75–7.05 (dd, 2H, $J = 7.2$ Hz, Ar-H), 7.13–7.30 (dd, 2H, $J = 7.5$ Hz, Ar-H), 7.56–7.83 (m, 4H, Ar-H), 9.31 (s, 1H, N-H). ^{13}C NMR (DMSO- d_6 , 300 MHz, δ ppm): 49.1 ($-\text{CH}_2$), Ar-C {119.2, 120.4, 122.2,

125.1, 127.4, 135.8, 137.1, 152.9, 158.9, 163.1, 166.8}, 194.5 ($\text{C}=\text{O}$). MS m/z (%): 368.04, Anal. Calcd for $\text{C}_{17}\text{H}_{12}\text{N}_4\text{O}_2\text{S}_2$ (368.4): C, 55.42; N, 15.21; H, 3.28; O, 8.69; S, 17.41%. Found: C, 54.04; N, 13.65; H, 3.09; O, 7.99; S, 16.99%.

4.2.11. Synthesis of S-1,3-Benzothiazol-2-yl-(benzylamino)ethanethionate (2j). White amorphous solid with m.p. 125 °C; yield (76%), pet. ether/ethyl acetate (2:3). IR (KBr, cm^{-1}): 2973 (CH_2), 1641 ($\text{C}=\text{O}$), 1090 ($\text{C}-\text{N}$), 1410 ($\text{C}=\text{C}$) 838 ($\text{C}-\text{S}$), 1276 ($\text{C}=\text{S}$), 1460 ($\text{C}=\text{N}$), 1345 ($\text{C}-\text{O}$). ^1H NMR: δ 3.36 (s, 2H, $-\text{CH}_2$), 3.90 (s, 2H, $-\text{CH}_2$), 6.50–6.70 (m, 5H, Ar-H), 7.25–7.80 (m, 4H, Ar-H), 9.15 (s, 1H, N-H). ^{13}C NMR (DMSO- d_6 , 300 MHz, δ ppm): 49.2 ($-\text{CH}_2$), 53.5 ($-\text{CH}_2$), Ar-C {65.8, 121.8, 122.5, 123.4, 125.8, 126.5, 128.5, 134.5, 147.0, 153.2, 161.3}, 193.3 ($\text{C}=\text{O}$). MS m/z (%): 314.05, Anal. Calcd for $\text{C}_{16}\text{H}_{14}\text{N}_2\text{O}$ (314.4): C, 61.12; N, 8.91; H, 4.49; O, 5.09; S, 20.40%. Found: C, 61.04; N, 7.65; H, 4.09; O, 4.97; S, 19.92%.

4.3. Antimicrobial Assay. Antimicrobial activities of the synthesized compounds 2(a–j) were studied against bacterial species (*S. pyogenes* ATCC 12346, *K. pneumonia* ATCC 13883, *E. coli* ATCC 25922, *S. typhi* ATCC 14028, *B. subtilis* ATCC 6051, and *S. aureus* ATCC 25923) using the agar well diffusion methodology with nutrient agar (Merck).³¹ The test sample and standard were taken in the concentration of 25 $\mu\text{g}/100 \mu\text{L}$. Levofloxacin was used as the standard antibacterial drug. The zones of inhibition caused by the standard and test samples were recorded in millimeters (mm). Further zones of inhibition for the most active compounds among the synthesized series of acetamide 2-mercaptobenzothiazole derivatives were measured at another two concentrations (50 and 75 $\mu\text{g}/100 \mu\text{L}$) and their MIC values were calculated.

4.4. Antibiofilm Activity. Biofilm inhibition assay was performed to determine the effect of the test samples (50 $\mu\text{g}/100 \mu\text{L}$ and 100 $\mu\text{g}/100 \mu\text{L}$) on the initial attachment of bacterial cells by using previously described procedures with few modifications.³² A 24-h fresh culture of test organisms (*S. aureus* and *K. pneumonia*) was obtained by subculturing onto nutrient agar plates and incubating at 37 °C for 24 h. After the fresh cultures were obtained, a bacterial suspension of the test organisms was prepared by suspending the test strains in nutrient broth. After that, 150 μL of the standardized bacterial inoculum (10^8 CFU/mL) and 100 μL of each of the test samples were introduced into the 96-well microliter plate. The well containing only the bacterial suspension was marked as the control. 100 μL each of cefadroxil (5 $\mu\text{g}/\mu\text{L}$) and DMSO was introduced into different wells of microliter plates containing the bacterial inoculum for determining their ability to inhibit biofilm formation. A well with un-inoculated nutrient broth was also prepared as an additional sterility control to ensure the sterility of the medium during the experiment. The plates were then sealed and incubated at 37 °C for 24 h under static conditions to allow the microbial cells to adhere to the surface of the plates. Following the incubation, the planktonic cells from the plates were gently removed and the wells were washed three times with PBS (pH 7.3). The bacterial cells still adhering to the plate were fixed by using 200 μL of 99% methanol for 15 min. The plates were then emptied and were allowed to dry. Subsequently, the plates were stained with 200 μL of 1% (w/v) crystal violet in each of the wells for 20 min. After staining, excess stain was removed by rinsing the plates thrice with PBS (pH 7.3). The plates were then air-dried, followed by re-solubilizing of the dye bound to the adherent

microorganisms with 200 μL of 33% (v/v) glacial acetic acid per well, and the optical density of each well was recorded at 595 nm using a Multiskan plate reader. The antibiofilm activity of the biofilm inhibitor compounds was determined based on the following formula

$$\text{anti - biofilm activity(\%)} = [1 - (\text{OD}_c)/\text{OD}_0] \times 100$$

where OD_c is the optical density of the well with the antibiofilm compound and pathogen, and OD_0 is the optical density of the pathogen suspension with no antibiofilm compound (control). The assay was performed in duplicate and the mean optical density was calculated.

4.5. Docking Studies of the Synthesized Compounds 2(a–j). The ligands were sketched in Discovery Studio Visualizer. The protein structures were downloaded from the protein data bank and were cleaned using Discovery Studio Visualizer. Both ligands and clean protein (pdb) files were converted to (pdbqt) format using AutoDock tools.³³ The binding pocket of the co-crystallized ligand was selected for docking in each case. The docking was performed using AutoDock Vina²³ and the results were visualized using Discovery Studio Visualizer, UCSF Chimera, and PyMOL.

AUTHOR INFORMATION

Corresponding Author

Humaira Nadeem – Department of Pharmaceutical Chemistry, Riphah Institute of Pharmaceutical Sciences, Riphah International University, Islamabad 44000, Pakistan; orcid.org/0000-0002-0169-0811; Email: humaira.nadeem@riphah.edu.pk

Authors

Ahmed Sadiq Sheikh – Department of Pharmaceutical Chemistry, Riphah Institute of Pharmaceutical Sciences, Riphah International University, Islamabad 44000, Pakistan

Muhammad Tariq Khan – Faculty of Pharmacy, Capital University of Science and Technology, Islamabad 44000, Pakistan

Adil Saeed – Department of Pharmaceutical Chemistry, Riphah Institute of Pharmaceutical Sciences, Riphah International University, Islamabad 44000, Pakistan; orcid.org/0000-0003-1433-8574

Babar Murtaza – Department of Pharmaceutical Chemistry, Riphah Institute of Pharmaceutical Sciences, Riphah International University, Islamabad 44000, Pakistan; orcid.org/0000-0003-1728-1120

Complete contact information is available at:

<https://pubs.acs.org/10.1021/acsomega.2c05782>

Notes

The authors declare no competing financial interest.

ACKNOWLEDGMENTS

The authors are thankful to the Department of Pharmaceutical Chemistry, Riphah Institute of Pharmaceutical Sciences, Riphah International University, Islamabad, Pakistan, Dr. Safia Ahmed, Pharmacy Department, Quaid-e-Azam University Islamabad, and Faculty of Pharmacy, Capital University of Science and Technology, Islamabad, Pakistan.

REFERENCES

(1) Panda, S. S.; Liaqat, S.; Girgis, A. S.; Samir, A.; Hall, C. D.; Katriitzky, A. R. Novel antibacterial active quinolone–fluoroquinolone

conjugates and 2D-QSAR studies. *Bioorg. Med. Chem. Lett.* **2015**, *25*, 3816–3821.

(2) Alizadeh, A.; Ghanbaripour, R.; Zhu, L.-G. Piperidine–iodine a dual system catalyst for synthesis of coumarin bearing pyrrolo [1, 2-a] quinoxaline derivatives via a one-pot three-component reaction. *Tetrahedron* **2014**, *70*, 2048–2053.

(3) Rouf, A.; Tanyeli, C. Bioactive thiazole and 2-mercaptobenzothiazole derivatives. *Eur. J. Med. Chem.* **2015**, *97*, 911–927.

(4) Shaaban, M. R.; Saleh, T. S.; Mayhoub, A. S.; Mansour, A.; Farag, A. M. Synthesis and analgesic/anti-inflammatory evaluation of fused heterocyclic ring systems incorporating phenylsulfonyl moiety. *Bioorg. Med. Chem.* **2008**, *16*, 6344–6352.

(5) Cogo, J.; Kaplum, V.; Sangi, D. P.; Ueda-Nakamura, T.; Correa, A. G.; Nakamura, C. V. Synthesis and biological evaluation of novel 2, 3-disubstituted quinoxaline derivatives as antileishmanial and antitrypanosomal agents. *Eur. J. Med. Chem.* **2015**, *90*, 107–123.

(6) Nikalje, A. P. G.; Deshpande, D.; Une, H. D. Facile synthesis and in vivo hypoglycemic activity of novel 2, 4-thiazolidinedione derivatives. *Eur. J. Exp. Biol.* **2012**, *2*, 343–353.

(7) Monisha, E.; Suganya, V.; Anuradha, V.; Syed Ali, M. Antioxidant, anti-inflammatory and antidiabetic activity of some novel chalcone and piperidine derivatives. *Int. Res. J. Pharmacy Med. Sci.* **2018**, *2*, 2581–3277.

(8) Borik, R. M.; Fawzy, N. M.; Abu-Bakr, S. M.; Aly, M. S. Design, synthesis, anticancer evaluation and docking studies of novel heterocyclic derivatives obtained via reactions involving curcumin. *Molecules* **2018**, *23*, 1398.

(9) Bondock, S.; Fadaly, W.; Metwally, M. A. Enaminonitrile in heterocyclic synthesis: Synthesis and antimicrobial evaluation of some new pyrazole, isoxazole and pyrimidine derivatives incorporating a 2-mercaptobenzothiazole moiety. *Eur. J. Med. Chem.* **2009**, *44*, 4813–4818.

(10) De Rosa, M.; Verdino, A.; Soriente, A.; Marabotti, A. An overview of Beta-Lactam antibiotics bearing more than one pharmacophoric group. *Int. J. Mol. Sci.* **2021**, *22*, 617.

(11) Shaista, A.; Amrita, P. 2-mercaptobenzothiazole-A magic molecule. *Int. J. Pharm. Sci. Res.* **2017**, *8*, 4909–4929.

(12) Nagarajan, S. R.; De Crescenzo, G. A.; Getman, D. P.; Lu, H.-F.; Sikorski, J. A.; Walker, J. L.; McDonald, J. J.; Houseman, K. A.; Kocan, G. P.; Kishore, N. Discovery of novel 2-mercaptobenzothiazolesulfonamides as potent inhibitors of HIV-1 protease. *Bioorg. Med. Chem.* **2003**, *11*, 4769–4777.

(13) Shafi, S.; Alam, M. M.; Mulakayala, N.; Mulakayala, C.; Vanaja, G.; Kalle, A. M.; Pallu, R.; Alam, M. Synthesis of novel 2-mercapto 2-mercaptobenzothiazole and 1, 2, 3-triazole based bis-heterocycles: their anti-inflammatory and anti-nociceptive activities. *Eur. J. Med. Chem.* **2012**, *49*, 324–333.

(14) Delmas, F.; Avellaneda, A.; Di Giorgio, C.; Robin, M.; De Clercq, E.; Timon-David, P.; Galy, J.-P. Synthesis and antileishmanial activity of (1, 3-benzothiazol-2-yl) amino-9-(10H)-acridinone derivatives. *Eur. J. Med. Chem.* **2004**, *39*, 685–690.

(15) Patil, V. S.; Nandre, K. P.; Ghosh, S.; Rao, V. J.; Chopade, B. A.; Sridhar, B.; Bhosale, S. V.; Bhosale, S. V. Synthesis, crystal structure and antidiabetic activity of substituted (E)-3-(Benzo [d] thiazol-2-ylamino) phenylprop-2-en-1-one. *Eur. J. Med. Chem.* **2013**, *59*, 304–309.

(16) Kamal, A.; Reddy, K. S.; Khan, M. N. A.; Shetti, R. V.; Ramaiah, M. J.; Pushpavalli, S.; Srinivas, C.; Pal-Bhadra, M.; Chourasia, M.; Sastry, G. N. Synthesis, DNA-binding ability and anticancer activity of 2-mercaptobenzothiazole/benzoxazole–pyrrolo [2, 1-c][1, 4] benzodiazepine conjugates. *Bioorg. Med. Chem.* **2010**, *18*, 4747–4761.

(17) Amir, M.; Javed, S. A.; Hassan, M. Z. Synthesis and antimicrobial activity of pyrazolinones and pyrazoles having 2-mercaptobenzothiazole moiety. *Med. Chem. Res.* **2012**, *21*, 1261–1270.

(18) Woodford, N. Biological counterstrike: antibiotic resistance mechanisms of Gram-positive cocci. *Clin. Microbiol. Infect.* **2005**, *11*, 2–21.

(19) Kumar, M.; Sarma, D. K.; Shubham, S.; Kumawat, M.; Verma, V.; Nina, P. B.; Jp, D.; Kumar, S.; Singh, B.; Tiwari, R. R. Futuristic Non-antibiotic Therapies to Combat Antibiotic Resistance: A Review. *Front. Microbiol.* **2021**, *12*, No. 609459.

(20) Liu, Y.; Shi, L.; Su, L.; Mei, H. C.; Van Der, J. P. C.; Ren, Y. Nanotechnology-based antimicrobials and delivery systems for biofilm infection control. *Chem. Soc. Rev.* **2019**, 428–446.

(21) Elbourne, A.; Truong, V. K.; Cheeseman, S.; Rajapaksha, P.; Gangadoo, S.; Chapman, J. The Use of Nanomaterials for the Mitigation of Pathogenic Biofilm Formation. In *Methods in Microbiology*; Academic Press, 2019; Vol. 46, pp 61–96.

(22) Tratat, C.; Petrou, A.; Geronikaki, A.; Theodoroula, N. F.; Haroun, M. Thiazolidin-4-Ones as Potential Antimicrobial Agents: Experimental and In Silico Evaluation. *Molecules* **2022**, *27*, 1930.

(23) Toshimitsu, A.; Terao, K.; Uemura, S. Intramolecular amidoselection of N-alkenyl amides: formation of nitrogen heterocycles. *J. Org. Chem.* **1986**, *51*, 1724–1729.

(24) Franchini, C.; Muraglia, M.; Corbo, F.; Florio, M. A.; Di Mola, A.; Rosato, A.; Matucci, R.; Nesi, M.; Van Bambeke, F.; Vitali, C. Synthesis and biological evaluation of 2-mercapto-1, 3-benzothiazole derivatives with potential antimicrobial activity. *Arch. Pharm.* **2009**, *342*, 605–613.

(25) Haroun, M.; Tratat, C.; Petrou, A.; Geronikaki, A.; Ivanov, M.; Ćirić, A.; Soković, M.; Nagaraja, S.; Venugopala, K. N.; Balachandran Nair, A.; Elsewedy, H.S.; Kochkar, H. Exploration of the antimicrobial effects of benzothiazolylthiazolidin-4-one and in silico mechanistic investigation. *Molecules* **2021**, *26*, 4061.

(26) Zheng, Z.; Liu, Q.; Kim, W.; Tharmalingam, N.; Fuchs, B. B.; Mylonakis, E. Antimicrobial activity of 1,3,4-oxadiazole derivatives against planktonic cells and biofilm of *Staphylococcus aureus*. *Future Med. Chem.* **2018**, *10*, 283–296.

(27) Miquel, S.; Lagrèfeuille, R.; Souweine, B.; Forestier, C. Anti-biofilm activity as a health issue. *Front. Microbiol.* **2016**, *7*, No. 592.

(28) Rashid, U.; Ahmad, W.; Hassan, S. F.; Qureshi, N. A.; Niaz, B.; Muhammad, B.; Imdad, S.; Sajid, M. Design, synthesis, antibacterial activity and docking study of some new trimethoprim derivatives. *Bioorg. Med. Chem. Lett.* **2016**, *26*, 5749–5753.

(29) Hosamani, K. M.; Shingalapur, R. V. Synthesis of 2-Mercaptobenzimidazole Derivatives as Potential Anti-microbial and Cytotoxic Agents. *Arch. Pharm.* **2011**, *344*, 311–319.

(30) Kumar, S.; Lim, S. M.; Ramasamy, K.; Vasudevan, M.; Shah, S. A. A.; Narasimhan, B. Bis-pyrimidine acetamides: design, synthesis and biological evaluation. *Chem. Cent. J.* **2017**, *11*, No. 80.

(31) Ghorab, M. M.; Alsaïd, M. S.; El-Gaby, M. S.; Elaasser, M. M.; Nissan, Y. M. Antimicrobial and anticancer activity of some novel fluorinated thiourea derivatives carrying sulfonamide moieties: synthesis, biological evaluation and molecular docking. *Chem. Cent. J.* **2017**, *11*, No. 32.

(32) Zalaru, C.; Dumitrascu, F.; Draghici, C.; Tarcomnicu, I.; Marinescu, M.; Nitulescu, G. M.; Chifiriuc, M. C.; et al. New Pyrazolo-Benzimidazole Mannich Bases with Antimicrobial and Antibiofilm Activities. *Antibiotics* **2022**, *11*, 1094.

(33) Trott, O.; Olson, A. J. AutoDock Vina: improving the speed and accuracy of docking with a new scoring function, efficient optimization, and multithreading. *J. Comput. Chem.* **2010**, *31*, 455–461.